

The origin of Franson-type nonlocal correlation

Byoung S. Ham

School of Electrical Engineering and Computer Science, Gwangju Institute of Science and Technology,
123 Chumdangwagi-ro, Buk-gu, Gwangju 61005, S. Korea
(Oct. 03, 2022)

Abstract: Franson-type nonlocal correlation results in a second-order intensity fringe between two remotely separated parties via coincidence measurements, whereas the corresponding local measurements show a perfect incoherence feature. This nonlocal correlation fringe between paired photons is mysterious due to the local randomness in both parties. Here, the Franson nonlocal correlation fringe is analytically investigated using the wave nature of photons to understand the mysterious quantum feature. As a result, the nonlocal intensity fringe is turned out to be a measurement selection-based coherence feature, while the local randomness is from effective decoherence among broad bandwidth-distributed photon pairs. As a result, a coherence version of Franson nonlocal correlation is suggested for macroscopic quantum applications with a commercial laser. The local and nonlocal correlations of the proposed scheme show the same results as entangled photon-pair based Franson correlation.

Introduction

Quantum entanglement is known as a weird phenomenon that cannot be explained by classical physics or achieved by any classical means [1]. Ever since the well-known thought experiment by Einstein, Podolsky and Rosen (EPR) in 1935 [2], EPR has been a key aspect of quantum information science and technologies in computing [3-5], communications [6-9] and sensing areas [10-12]. Although Bell has mathematically demonstrated the so-called EPR paradox in 1964, the definition of classical physics rules out coherence optics [13]. Since then, mutual coherence between paired photons has not been carefully considered [13-26]. Although the energy-time uncertainty relation prohibits definite phase information for a single photon, a mutual phase between entangled photons is free from such uncertainty relation without violating quantum mechanics. Here, we focus on the mutual coherence between interacting photons in Franson-type nonlocal correlation to understand the mysterious quantum feature. The classical understanding stands for a definite and clear reasoning-based physical nature.

Franson-type nonlocal correlation [19] has been studied since 1987 [20-26]. Unlike Bell inequality violations [13-18], Franson nonlocal correlation is based on a set of unbalanced Mach-Zehnher interferometers (U-MZIs) [19-26]. The U-MZI is designed with respect to interacting photons' bandwidth for both local randomness in each detector and nonlocal correlation fringe in coincidence detection. The local randomness-based nonlocal fringe is a unique feature of the Franson correlation. Although the mathematical form of the nonloal correlation is clear to view the fringe, the physical understanding of the nonlocal fringe has been severely limited. Thus, the fringe in Franson nonlocal correlation has been left as a mysterious quantum feature due to the U-MZI resulting local randomness. Here, the origin of Franson nonlocal correlation is investigated to clear out the weirdness of nonlocal fringe based on local randomness. For this, we analyze the relation between U-MZI and entangled photon pairs generated from spontaneous parametric down conversion (SPDC) process [27-31]. Specifically, the coherence relation between each entangled photon pair and the U-MZI is focused on for coincidence detection. From this understanding, a coherence version of the Franson correlation is proposed for macroscopic quantum information compatible with current technologies based on coherence optics.

Results

Figure 1 shows the original Franson scheme for nonlocal correlation using entangled photon pairs generated from SPDC processes [20]. As studied [29] and applied for quantum key distributions [24-26], the coincidence measurements between two remotely separated output photons show a path-length difference-dependent fringe, even though their local measurements do not. This nonlocal fringe for the second-order intensity correlation looks exactly

the same as the first-order intensity correlation in a typical double-slit case. Regarding the U-MZIs in Fig. 1(a), whose entangled photon source S is depicted in Figs. 1(b) and 1(c), the nonlocal correlation fringe due to the coincidence measurements implies that each U-MZI may act as a coherence system for individual photon pairs. Considering this, the coherence time τ_c of each entangled photon pair from the SPDC should be much longer than the path-length difference ΔL ($L - S$) of each U-MZI. This coherence relation can be achieved by choosing a narrow bandwidth pump laser (p) in Fig. 1(c) according to $\chi^{(2)}$ nonlinear optics of SPDC [20,30,31]. As explained below in equation (11), the coherence washout among the broadband photon pairs is suppressed by coincidence measurements. Due to the ultrawide bandwidth (Δ) of the entangled photon ensemble in Fig. 1(b), however, each U-MZI in Fig. 1(a) acts as a noninterfering interferometer for local measurements, resulting in the path-length independent uniform intensity. Thus, both local and nonlocal measurements are easily understood by many-wave interference in coherence optics.

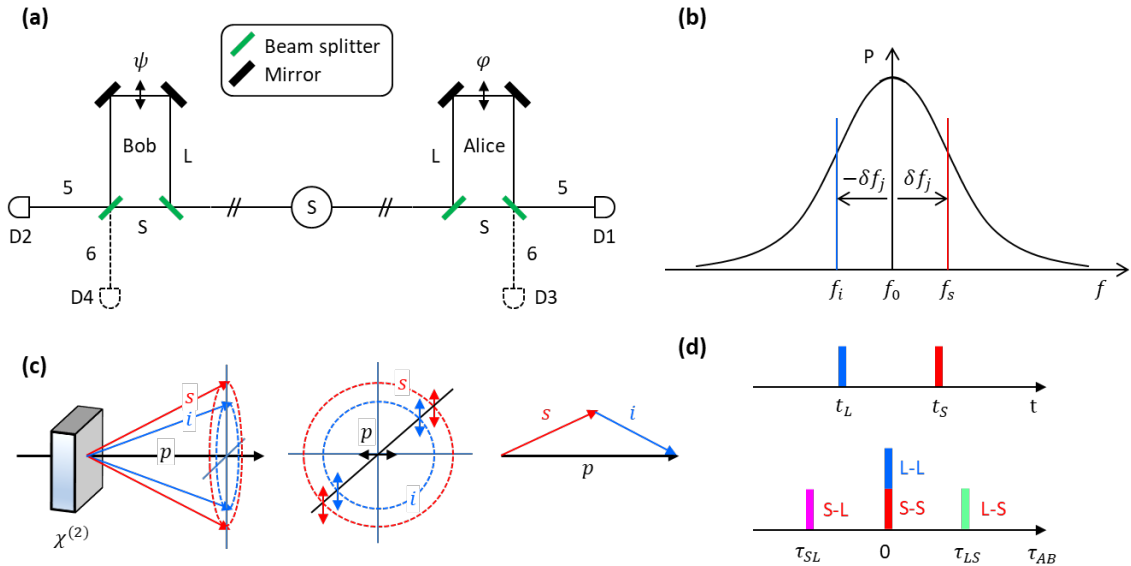


Fig. 1. Schematic of Franson-type nonlocal correlation. (a) The original Franson setup. (b) Probability distribution of the frequency of the light source S in (a). (c) Schematic of Type I SPDC. $2f_0 = f_s + f_i$. S (short path) and L (long path) indicate the two paths of each unbalanced MZI. (d) Schematic of coincidence detection. D: single photon detector. In (b), the full width at half maximum of entangled photons is Δ . In (c), p, s, and i indicate pump, signal, and idler photons, respectively, where s and i can be swapped due to the phase matching condition (see text).

For the U-MZI (Alice) in Fig. 1(a), coherence optics for each input photon E_0 results in the following matrix representation for the output photons:

$$\begin{bmatrix} E_5 \\ E_6 \end{bmatrix}_{Alice} = [BS][\varphi'] [BS] \begin{bmatrix} E_0 \\ 0 \end{bmatrix} \\ = \frac{1}{2} \begin{bmatrix} 1 + e^{i\varphi'_j} \\ i(1 - e^{i\varphi'_j}) \end{bmatrix}, \quad (1)$$

where $[BS] = \frac{1}{2} \begin{bmatrix} 1 & i \\ i & 1 \end{bmatrix}$, $[\varphi'_j] = \begin{bmatrix} 1 & 0 \\ 0 & -e^{i\varphi'_j} \end{bmatrix}$, and $\varphi'_j = \delta f_j \tau + \varphi$. Here, the amplitude of a single photon is set at E_0 , where a harmonic oscillation term is omitted for simplicity. τ is the temporal difference of the photon between L and S of the U-MZI, $\tau = (L - S)/c$, where c is the speed of light. δf_j is the detuning of the j^{th} photon pair with respect to the center frequency f_0 as shown in Fig. 1(b).

Figure 1(c) shows schematic of Type I SPDC for the same polarization of entangled photon pairs. Due to the phase matching condition of SPDC governed by both energy and momentum conservation laws [30,31], the signal

(s) and idler (i) photons are interchangeable, satisfying an entangled state, $|\psi\rangle = \frac{1}{\sqrt{2}}(|s\rangle_1|i\rangle_2 + |i\rangle_1|s\rangle_2)$, where the subscripts indicate concentric circles. Thus, the f_0 in Fig. 1(b) is the half of the pump photon frequency, whose spectral width is ultranarrow compared with the generated photon bandwidth Δ . Here, having a narrow linewidth pump laser is essential for the higher efficiency of nonlocal fringe visibility via stable concentric ring patterns in Fig. 1(c) according to the momentum conservation law [20,31,32]. According to the phase matching in SPDC nonlinear optics [31], the paired (signal and idler) photons satisfy symmetric frequency detuning (δf_j) across the center frequency f_0 , resulting in a $\pm\delta f_j$ relation with $2f_0 = f_s + f_i$ according to the energy conservation law [31].

Likewise, the matrix representation for Bob's side in Fig. 1(a) is as follows:

$$\begin{bmatrix} E_5 \\ E_6 \end{bmatrix}_{Bob} = \frac{1}{2} \begin{bmatrix} 1 + e^{i\psi'_j} \\ i(1 - e^{i\psi'_j}) \end{bmatrix}, \quad (2)$$

where $\psi'_j = -\delta f_j\tau + \psi$. As a result, the mean amplitudes of each output port in both sides are as follows:

$$E_{5j}^A = \frac{E_0}{2} \left(1 + e^{i\varphi'_j} \right), \quad (3)$$

$$E_{6j}^A = \frac{iE_0}{2} \left(1 - e^{i\varphi'_j} \right), \quad (4)$$

$$E_{5j}^B = \frac{E_0}{2} \left(1 + e^{i\psi'_j} \right), \quad (5)$$

$$E_{6j}^B = \frac{iE_0}{2} \left(1 - e^{i\psi'_j} \right). \quad (6)$$

In equations (3)-(6), the superscript A (B) indicates Alice (Bob), and the subscript 5 (6) is for the output port number. From equations (3)-(6), the corresponding mean intensities are as follows:

$$\langle I_{5j}^A \rangle = \langle \frac{I_0}{2} (1 + \cos \varphi'_j) \rangle, \quad (7)$$

$$\langle I_{6j}^A \rangle = \langle \frac{I_0}{2} (1 - \cos \varphi'_j) \rangle, \quad (8)$$

$$\langle I_{5j}^B \rangle = \langle \frac{I_0}{2} (1 + \cos \psi'_j) \rangle, \quad (9)$$

$$\langle I_{6j}^B \rangle = \langle \frac{I_0}{2} (1 - \cos \psi'_j) \rangle. \quad (10)$$

Thus, the ensemble average of local measurements becomes uniform at $\frac{I_0}{2}$ due to wide bandwidth Δ , resulting the local randomness. This uniform intensity in local detections is of course due to many-wave interference, satisfying the incoherence optics of U-MZIs. As a result, this no-fringe in local measurements can be easily understood as a direct result of coherence optics for photon ensemble average.

The mean coincidence measurements between remotely separated output photons, e.g., $\langle R_{5j}^{AB} \rangle$ ($= \langle I_{5j}^A I_{5j}^B \rangle$), are directly calculated from the product of equations (7) and (9):

$$\begin{aligned} \langle R_{5j}^{AB}(\tau) \rangle &= \langle \frac{I_0^2}{4} (1 + \cos \varphi'_j)(1 + \cos \psi'_j) \rangle \\ &= \langle \frac{I_0^2}{4} \{1 + \cos(\delta f_j\tau + \varphi) + \cos(-\delta f_j\tau + \psi) + \frac{1}{2} [\cos(\varphi + \psi) + \cos(2\delta f_j\tau + \varphi - \psi)]\} \rangle. \end{aligned} \quad (11)$$

In equation (11), the last two terms are related to the product of the coincidence detection. By definition of coincidence ($\tau = 0$), the last two terms in the bracket become equal for $\psi = 0$, regardless of δf_j . Here, the effective coherence time τ_c is Δ^{-1} . The τ_c -based coherence length l_c is much longer than the wavelength λ of each entangled photon. For coincidence detection ($\tau = 0$), equation (11) turns out to be φ -dependent (for $\psi = 0$):

$$\langle R_{55}^{AB}(\tau = 0; \varphi) \rangle = \frac{\langle I_0^2 \rangle}{4} (1 + \cos \varphi). \quad (12)$$

Equation (12) is the heart of Franson-type nonlocal correlation, where the fringe depends only on the path-length variation δL ($= |L_B - L_A|$) in U-MZIs. Due to the fine phase controllability of U-MZIs with δL , the bracket of the $\cos \varphi$ term is removed. This path-length dependent fringe in nonlocal correlation is originated in the particular measurement process of coincidence detection ($\tau = 0$), otherwise results in the classical lower bound, $\langle R_{55}^{AB} \rangle = \frac{\langle I_0^2 \rangle}{4} (1 + \frac{1}{2} \cos \varphi)$. This is the coherence interpretation of the Franson-type nonlocal correlation in the present analysis for a special case of $\psi = 0$.

Likewise, all other nonlocal correlations between the paired photons coincidentally measured for $\psi = 0$ in both parties are as follows:

$$\langle R_{56}^{AB} \rangle = \frac{\langle I_0^2 \rangle}{2} (1 - \cos \varphi), \quad (13)$$

$$\langle R_{66}^{AB} \rangle = \frac{\langle I_0^2 \rangle}{2} (1 + \cos \varphi), \quad (14)$$

$$\langle R_{65}^{BA} \rangle = \frac{\langle I_0^2 \rangle}{2} (1 - \cos \varphi). \quad (15)$$

Equations (12)-(15) are exactly the same as those observed in ref. 32 for loophole-free Franson correlation. Thus, the phase φ in equations (11)-(15) is nothing but for the path-length difference between two parties, $\delta L (= L_B - L_A)$. As a result, Franson-type nonlocal correlation can be considered as a special version of coherence optics via coincidence measurements. General coherence optics without a temporal (spectral) modification of the coincidence detection cannot result in this nonlocal property.

We now analyze the general case of the Franson-type nonlocal correlation for both independent parameters ψ and φ . In both U-MZIs of Fig. 1(a), each output photon can be represented by linear superposition of both paths of S and L, as shown in Eqs. (2)-(5), where S and L are omitted for simplicity. Thus, there are four different path-basis product combinations for nonlocal correlation measurements between space-like separated local U-MZIs. Firstly, the paired photons pass through only short paths in both parties, resulting in a S-S path relation. Secondly, the paired photons pass through only long paths, resulting in a L-L relation. Thirdly, the paired photons pass through either a short or long path, resulting in a S-L or L-S relation. In Fig. 1(d), the top plot is for photons measured in an absolute time domain, while the bottom plot is in a coincidence-time domain ($\tau = \tau_{AB}; \tau_{AB} = t_A - t_B$). For $\tau_{AB} = 0$, both S-S and L-L choices are permitted by the definition of coincidence detection, where the S-L and L-S choices are prohibited due to the ensemble incoherence feature given by $\Delta L \gg \Delta f_j c$, resulting in temporally separated wave packets. Thus, the coincidence process causes measurement modification, allowing S-S and L-L products only. This measurement-event modification by coincidence detection also induces indistinguishability between nonlocally measured photons. Here, indistinguishability is an essential condition for quantum superposition in the particle nature of quantum mechanics [1,3].

Using modified Eqs. (1)-(4) with path bases $|S\rangle_{A,B}$ and $|L\rangle_{A,B}$ (see Appendix), the amplitude E_{AB} of coincidentally measured nonlocal correlation $R_{AB}(\tau = 0)$ between two corresponding local measurements in Fig. 1(a) can be described as:

$$E_{5j}^{AB}(\tau = 0) = \frac{I_0}{4} e^{i\eta} \left(|SS\rangle_{AB} + |LL\rangle_{AB} e^{i(\varphi'_j + \psi'_j)} \right), \quad (16)$$

where both terms of $|SL\rangle_{AB}$ and $|LS\rangle_{AB}$ are ruled out by the definition of coincidence detection, as mentioned above (see Fig. 1(d)). Here, $R_{5j}^{AB} = E_{5j}^{AB} (E_{5j}^{AB})^*$ and $E_{5j}^{AB} = E_{5j}^A E_{5j}^B$. Equation (16) is the second-order superposition compared with the first-order superposition of Eqs. (1)-(4). Unlike Eq. (11), the term of E_{5j}^{AB} can never be achieved coherently without the coincidence detection at $\tau = 0$. This is the quintessence of the present interpretation of the Franson-type nonlocal correlation for the coincidence detection. As a result, the following nonlocal fringe is achieved for the j^{th} photon pair:

$$R_{5j}^{AB}(\tau = 0) = \frac{I_0^2}{8} (1 + \cos(\varphi'_j + \psi'_j)). \quad (17)$$

Due to the symmetric detuning of SPDC-generated entangled photon pair (see Fig. 1(b)), Eq. (17) is independent of δf_j of the j^{th} photon pair: $\varphi'_j + \psi'_j = \varphi + \psi$. Thus, the time averaged (mean) nonlocal correlation is only dependent on both U-MZI phase controls, regardless of the SPDC bandwidth:

$$\langle R_{55}^{AB}(\tau = 0) \rangle = \frac{\langle I_0^2 \rangle}{8} (1 + \cos(\varphi + \psi)). \quad (18)$$

On the contrary of Eq. (12), Eq. (18) is the general form of the coherence interpretation for the Franson-type nonlocal correlation in an inseparable intensity product manner between two local measurements, resulting in nonlocal phase correlation. Assuming well stabilized U-MZIs in both parties, thus, the mysterious nonlocal fringe in

the Franson scheme is successfully analyzed using the wave nature of photons for the coincidence detection. Here, the indistinguishability between coincidence detection-resulting path-basis products in Eq. (16) plays an essential role for the joint phase control of $\cos(\varphi + \psi)$ in Eq. (18).

Over the last several decades, Franson-type nonlocal correlation has been applied to quantum key distributions based on the energy-time bin method using single photon-correlated entangled pairs [24-26]. Because this nonlocal phenomenon is successfully explained by coherence optics for coincidence measurements in equation (18), a coherence version of the Franson-type nonlocal correlation can be considered as well. In quantum mechanics, the believed thumb rule is that nonlocal correlation cannot be achieved by any classical means. Thus, the present analysis provides some insight into the quantum nature.

Figure 2 shows a coherence version of Fig. 1, where the entangled photon pairs are replaced by coherent photons from a commercial laser with some modifications. Unlike the SPDC-generated entangled photon pairs, the spectral bandwidth Δ_l of each coherent photon is the same as the laser linewidth according to cavity optics [33]. To satisfy both temporal and spectral integrations for nonlocal and local measurements, respectively, the laser-generated photons are modified to be inhomogeneously broadened. This inhomogeneity (Δ) of coherent photons is conducted by a synchronized pair of acousto-optic modulators (AOMs), resulting in the same function of overall decoherence in ensemble measurements of SPDC. Such spectral widening of coherent photons can also be accomplished by frequency modulation of continuous waves [34] or dc Stark effects [35].

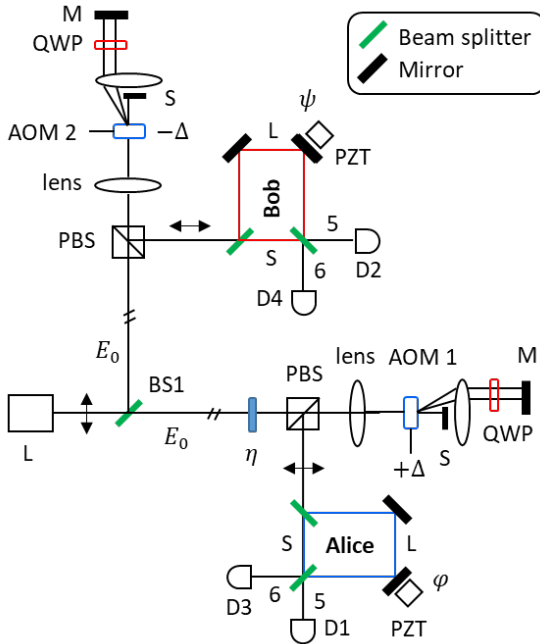


Fig. 2. Schematic of a coherence version of Franson nonlocal correlation. AOM: acousto-optic modulator. D: photo detector. SM: spectral modifier, S: beam stopper.

For random distributions of individual detuning δf_j within 2Δ bandwidth in a double-pass AOM scheme via a quarter-wave plate (QWP) for a polarization rotation, the AOM's scanning speed should be much faster than the generation rate of photon pairs for a Δ_j -dependent random phase. Thus, the AOM-generated Δ_j ($= \delta f_j \tau$)-detuned coherent-photon pairs in Fig. 2 have the signal and idler photon-pair relation in SPDC processes. For each doubly-bunched photon pair according to Poisson statistics, a phase shift η is added into one party (Bob). However, this η does not affect the MZI physics for the output photons. In the U-MZIs in both parties, the matrix representations for the j^{th} output photons are as follows:

$$E_{5j}^A = \frac{E_0}{2} e^{i(\Delta_j + \Delta_S)} (|S\rangle_A + e^{i\Delta_{LS}} |L\rangle_A e^{i\varphi_j'}), \quad (19)$$

$$E_{6j}^A = \frac{E_0}{2} e^{i(\Delta_j + \Delta_S)} (|S\rangle_A - e^{i\Delta_{LS}} |L\rangle_A e^{i\varphi_j'}), \quad (20)$$

$$E_{5j}^B = \frac{E_0}{2} e^{-i(\Delta_j - \Delta_S - \eta)} (|S\rangle_B + e^{i\Delta_{LS'}} |L\rangle_B e^{i\psi_j'}), \quad (21)$$

$$E_{6j}^B = \frac{E_0}{2} e^{-i(-\Delta_j - \Delta_S - \eta)} (|S\rangle_B - e^{i\Delta_{LS'}} |L\rangle_B e^{i\psi_j'}), \quad (22)$$

where $\Delta_{LS} = \Delta_L - \Delta_S$ is the difference path length-induced phase difference in the U-MZI at Alice's side, and Δ_{LS}' is the corresponding one at Bob's side. As mentioned above for the general analysis of the nonlocal correlation, $\varphi_j' = \delta f_j + \varphi$ and $\psi_j' = -\delta f_j \tau + \psi$ are also obtained by classically controlled AOMs in Fig. 2. For an appropriate mean photon number much less than unity, the doubly bunched photon pair at \sim kHz rate can be easily provided using an attenuated laser [33]. Thus, the AOM scan speed at \sim MHz results in random phase distribution in both φ_j' and ψ_j' . The absolute short-path lengths of the U-MZIs are slightly different, resulting in $\Delta_{LS}' \neq \Delta_{LS}$. Each long paths are controlled by piezo-electric transducers (PZTs), resulting in a definite values of φ and ψ . Thus, the corresponding local intensities are as follows:

$$I_{5j}^A = \frac{I_0}{2} (1 + \cos(\Delta_{LS} + \varphi_j')), \quad (23)$$

$$I_{6j}^A = \frac{I_0}{2} (1 - \cos(\Delta_{LS} + \varphi_j')), \quad (24)$$

$$I_{5j}^B = \frac{I_0}{2} (1 + \cos(\Delta_{LS}' + \psi_j')), \quad (25)$$

$$I_{6j}^B = \frac{I_0}{2} (1 - \cos(\Delta_{LS}' + \psi_j')). \quad (26)$$

The results of Eqs. (23)-(26) are basically the same as Eqs. (7)-(10), because Δ_{LS} and Δ_{LS}' are fixed.

For the mean value of the local measurements in each output port, the bandwidth Δ of the AOMs plays an essential role according to the MZI physics via linear superposition. For the coherence feature of each photon pair in both U-MZIs, the first condition of $\delta f_L \ll \Delta$ and $\frac{c}{\delta f_L} \gg \Delta_{LS}$ must be met, as analyzed in Fig. 1, where δf_L is the linewidth of the laser L. For the ensemble of photon pairs, the second condition of $\frac{c}{\Delta} \ll \Delta_{LS}$ must be met, too. Under these conditions, mean measurements of Eqs. (23)-(26) become unity, satisfying local randomness:

$$\langle I_k^P \rangle = \langle \sum_{j=0}^N I_{kj}^P \rangle = \frac{\langle I_0 \rangle}{2}, \quad (27)$$

where $k = 5, 6$ and $P=A, B$.

The presumed nonlocal correlation between local measurements of space-like separated parties is as follows:

$$\begin{aligned} R_{5j}^{AB}(\tau) &= I_{5j}^A(\tau) I_{5j}^B(\tau) \\ &= \frac{I_0^2}{4} (1 + \cos(\Delta_{LS} + \varphi_j')) (1 + \cos(\Delta_{LS}' + \psi_j')). \end{aligned} \quad (28)$$

Equation (28) is the direct result of the intensity product between two individual measurements without τ information of coincidence detection. The role of the coincidence detection is for measurement modification in Franson-type nonlocal correlation as derived above in Fig. 1. Thus, Eq. (28) belongs to classical physics, where the measurement basis product is separable. If coincidence detection is applied to Eq. (28), however, only S-S and L-L measurement-basis products are selectively chosen, resulting in the second-order nonlocal amplitude correlation, $E_{kj}^{AB} (= E_{kj}^A E_{kj}^B)$, as shown in Eq. (16). Thus, $R_{5j}^{AB}(\tau) = E_{5j}^{AB} (E_{5j}^{AB})^*$ is obtained as a quantum feature via coincidence detection:

$$\begin{aligned} R_{5j}^{AB}(\tau = 0) &= \frac{I_0^2}{16} e^{-i2\Delta_j} e^{i(2\Delta_S + \eta)} (|S\rangle_A + e^{i\Delta_{LS}} |L\rangle_A e^{i\varphi_j'}) (|S\rangle_B + e^{i\Delta_{LS'}} |L\rangle_B e^{i\psi_j'}) (c.c.) \\ &= \frac{I_0^2}{8} (1 + \cos((\Delta_{LS} + \Delta_{LS}' + \psi_j' + \varphi_j'))), \end{aligned} \quad (29)$$

where c.c. is complex conjugate. Due to $\psi_j' + \varphi_j' = \psi + \varphi$ regardless of Δ and a fixed value of $\Delta_{LS} + \Delta_{LS}' (= \xi)$, the joint phase-dependent Franson-type nonlocal correlation is achieved:

$$\langle R_{55}^{AB}(\tau = 0) \rangle = \frac{\langle I_0^2 \rangle}{8} (1 + \cos(\xi + \psi + \varphi)). \quad (30)$$

Likewise,

$$\langle R_{66}^{AB}(\tau = 0) \rangle = \frac{\langle I_0^2 \rangle}{8} (1 - \cos(\xi + \psi + \varphi)). \quad (31)$$

Equations (30) and (31) show the same fringes as observed in the typical Franson-type nonlocal correlations using SPDC-generated entangled photon pairs [20,32]. Thus, a classical model of the Franson-type nonlocal correlation is successfully presented for quantum features using the wave nature of photons without violating quantum mechanics.

Conclusion

Franson-type nonlocal correlation was analyzed and discussed using the wave nature of photons for both local randomness and nonlocal correlation fringe. For this, the original unbalanced MZI (U-MZI) is investigated with respect to the characteristics of entangled photons generated from Type I SPDC. From this, the locally measured uniform intensity in each detector was analyzed as a dephasing effect due to many-wave interference of spectrally broadened photons. On the contrary, the U-MZI path-length dependent intensity fringe for the nonlocal correlation was analyzed as a coherence feature of each photon pair in the U-MZI, where the U-MZI is designed to be coherent with respect to each photon pair. This coherence condition is satisfied with a narrow-bandwidth pump laser via coincidence detection. Unlike local measurements in time averaging, resulting in overall decoherence, the nonlocal measurements require coincidence detection between two remotely separated local measurements. This coincidence detection is key to understand the nonlocal fringe due to ruling out noncoincidence events, resulting in measurement modification. Thus, the origin of both local randomness and nonlocal Franson correlation was found in coherence optics, where the nonlocal property is due to measurement filtering via coincidence detections. Based on this understanding, a coherence version of Franson nonlocal correlation was proposed using spectral modification of a commercially available laser light for the local randomness. The nonlocal correlation was achieved using a pair of acousto-optic modulators mimicking the SPDC-generated signal and idler photon pairs in symmetric frequency detuning.

Appendix

In general, the amplitude of an arbitrary j^{th} output photon from the U-MZI of Alice can be represented coherently according to the wave nature of photons in quantum mechanics:

$$E_{5j}^A = \frac{E_0}{2} \left(|S\rangle_A + |L\rangle_A e^{i\varphi'_j} \right), \quad (A1)$$

$$E_{6j}^A = \frac{iE_0}{2} \left(|S\rangle_A - |L\rangle_A e^{i\varphi'_j} \right), \quad (A2)$$

where $\varphi'_j = \delta f_j \tau + \varphi$, and the notations of $|S\rangle_A$ and $|L\rangle_A$ denote unit vectors of a photon state propagating along the short (S) and long (L) paths of the U-MZI at Alice's side, respectively. E_0 is the amplitude of a single photon. In the same way, the output photons from the U-MZI at Bob's side can also be described coherently with respect to Eqs. (A1) and (A2):

$$E_{5j}^B = \frac{E_0}{2} e^{i\eta} \left(|S\rangle_B + |L\rangle_B e^{i\psi'_j} \right), \quad (A3)$$

$$E_{6j}^B = \frac{iE_0}{2} e^{i\eta} \left(|S\rangle_B - |L\rangle_B e^{i\psi'_j} \right), \quad (A4)$$

where $\psi'_j = -\delta f_j \tau + \psi$, and η is the relative phase caused by the path-length difference between U-MZIs from the source L.

Acknowledgement

This work was supported by the ICT R&D program of MSIT/IITP (2021-0-01810), via Development of Elemental Technologies for Ultra-secure Quantum Internet.

Reference

1. Brunner, N. et al. Bell nonlocality. *Rev. Mod. Phys.* **86**, 419–478 (2014).

2. Einstein, A., Podolsky, B. & Rosen, N. Can quantum-mechanical description of physical reality be considered complete? *Phys. Rev.* **47**, 777-780 (1935).
3. F. Arute, et al., Quantum supremacy using programmable superconducting processor. *Nature* **574**, 505-510 (2019).
4. H.-S. Zhong et al., Phase-programmable Gaussian Boson sampling using stimulated squeezed light. *Phys. Rev. Lett.* **127**, 180502 (2021).
5. S. Ebadi et al., Quantum phases of matter on a 256-atom programmable quantum simulator. *Nature* **595**, 227-232 (2021).
6. Y.-A. Chen et al., An intergrated space-to-ground quantum communication network over 4,600 kilometres. *Nature* **589**, 214-219 (2021).
7. B. Korzh, C. C. W. Lim, R. Houlmann, N. Gisin, M. J. Li, D. Nolan, B. Sanguinetti, R. Thew, H. Zbinden, Provably secure and practical quantum key distribution over 307 km of optical fibre. *Nat. Photonics* **9**, 163–168 (2015).
8. P. Sibson et al., Chip-based quantum key distribution. *Nat. Communi.* **8**, 13984 (2017).
9. I. Marcikic, H. de Riedmatten, W. Tittel, H. Zbinden, M. Legre, and N. Gisin, Distribution of time-bin entangled qubits over 50 km of optical fiber. *Phys. Rev. Lett.* **93**, 180502 (2004).
10. Giovannetti, V., Lloyd, S. & Maccone, L. Advances in quantum metrology. *Nature Photon.* **5**, 222-229 (2011).
11. C. L. Degen, F. Reinhard, and P. Cappellaro, Quantum sensing. *Rev. Mod. Phys.* **89**, 035002 (2017).
12. Dowling, J. P. Quantum optical technologies for metrology, sensing, and imaging. *J. Lightwave Tech.* **33**, 2359-2370 (2015).
13. Bell, J. On the Einstein Podolsky Rosen Paradox. *Physics* **1**, 195-290 (1964).
14. Clauser, J. F., Horne, M. A., Shimony, A. & Holt, R. A. Proposed experiment to test local hidden-variable theories. *Phys. Rev. Lett.* **23**, 880–884 (1969).
15. X.-S. Ma, A. Qarry, J. Kofler, T. Jennewein, and A. Zeilinger. Experimental violation of a Bell inequality with two different degree of freedom of entangled particle pairs. *Phys. Rev. A* **79**, 042101 (2009).
16. B. Hensen et al., Loophole-free Bell inequality violation using electron spins separated by 1.3 kilometres. *Nature* **526**, 682-686 (2015).
17. Clauser, J. F., Horne, M. A., Shimony, A. & Holt, R. A. Proposed experiment to test local hidden-variable theories. *Phys. Rev. Lett.* **23**, 880–884 (1969).
18. Żukowski, M., Zeilinger, A., Horne, M. A. & Ekert, A. K. “Event-ready-detectors” Bell experiment via entanglement swapping. *Phys. Rev. Lett.* **71**, 4287–4290 (1993).
19. J. D. Franson, Bell inequality for position and time. *Phys. Rev. Lett.* **62**, 2205-2208 (1989).
20. Kwiat, P. G., Steinberg, A. M. & Chiao, R. Y. High-visibility interference in a Bell-inequality experiment for energy and time. *Phys. Rev. A* **47**, R2472–R2475 (1993).
21. Aerts, S., Kwiat, P., Larsson, J.-Å. & Żukowski, M. Two-photon Franson-type experiments and local realism. *Phys. Rev. Lett.* **83**, 2872-2875 (1999).
22. A. Cabello, A. Rossi, G. Vallone, F. De Martini, and P. Mataloni, Proposed Bell experiment with genuine energy-time entanglement. *Phys. Rev. Lett.* **102**, 040401 (2009).
23. G. Carvacho et al., Postselection-loophole-free Bell test over an installed optical fiber network. *Phys. Rev. Lett.* **115**, 030503 (2015).
24. W. Tittel, J. Brendel, H. Zbinden, and N. Gisin, Violation of Bell inequality by photons more than 10 km apart. *Phys. Rev. Lett.* **81**, 3563-3566 (1998).
25. Boaron, A. et al. Simple 2.5 GHz time-bin quantum key distribution. *Appl. Phys. Lett.* **112**, 171108 (2018).
26. Cuevas, A. et al. Long-distance distribution of genuine energy-time entanglement. *Nature Communi.* **4**, 2871 (2013).
27. R. W. Boyd, *Nonlinear Optics, Third Edition*. New York (Academic Press, 2008) pp. 79–88.
28. H. Defienne and S. Gigan, Spatially entangled photon-pair generation using a partial spatially coherent pump beam. *Phys. Rev. A* **99**, 053831 (2019).

29. O. Kwon, Y.-S. Ra, and Y.-H. Kim, Coherence properties of spontaneous parametric down-conversion pumped by a multi-mode cw diode laser. *Opt. Exp.* **17**, 13059-13069 (2009).
30. B. E. A. Saleh and M. C. Teich, *Fundamentals of photonics*. 2nd Ed. (Wiley, New York, NY, 2012), ch. 21.
31. H. Cruz-Ramirez, R. Ramirez-Alarcon, M. Corona, and K. Garay-Palmett, and A. B. U'Ren, Spontaneous parametric processes in modern optics. *Opt. Photon. News* **22**, 36-41 (2011), and reference therein.
32. G. Lima, G. Vallone, A. Chiuri, A. Cabello, and P. Mataloni, *Phys. Rev. A* **81**, 640101(R) (2010).
33. S. Kim and B. S. Ham, Revisiting self-interference in Young's double-slit experiments. arXiv:2104.08007 (2021).
34. Behroozpour, B., Sandborn, P., Wu, M. & Boser, B. E. Lidar system architectures and circuits. *IEEE Commun. Mag.* **55**, 135–142 (2017)
35. A. L. Alexander, J. J. Longdell, M. J. Sellars, and N. B. Manson, Photon echoes produced by switching electric fields. *Phys. Rev. Lett.* **96**, 043602 (2006).

Author contribution

B.S.H. solely wrote the manuscript. Correspondence and request of materials should be addressed to BSH (email: bham@gist.ac.kr).

Conflict of interest

The author has no conflicts to disclose.

Data availability

Data sharing not applicable – no new data generated.